PCCP

Accepted Manuscript

ROYAL SOCIETY OF CHEMISTRY

www.rsc.org/pccp

PCCP

RSCPublishing

PAPER

Electrical percolation threshold of semiconducting single-walled carbon nanotube networks on field-effect transistor

Cite this: DOI: 10.1039/xoxxoooooox

Received ooth January 2012,
Accepted ooth January 2012

DOI: 10.1039/xoxxoooooox

www.rsc.org/

Ho-Kyun Jang, Jun Eon Jin, Jun Hee Choi, Pil-Soo Kang, Do-Hyun Kim* and Gyu Tae Kim*

With the advance in separation and purification of carbon nanotube (CNT), using highly pure metallic or semiconducting CNT has practical merit in the application to electronics. When highly pure CNT is applied to various fields, CNT networks are preferred to an individual CNT. At this moment, the presence of an electrical path becomes crucial in the networks. In this study, we report on electrical percolation threshold of semiconducting single-walled carbon nanotube (s-SWCNT) networks and their electrical characteristics in field-effect transistor (FET). By Monte Carlo method, the networks of s-SWCNT were randomly generated in the channel defined by source-drain electrodes of FET. On the basis of percolation theory, percolation threshold of s-SWCNT networks was obtained at different channel lengths (2, 6, and 10 μm) by generating random s-SWCNT networks 100 times. The network density corresponding to electrical percolation threshold was theoretically gained at each channel length. As a result, the network densities at percolation threshold in the channel length of 2, 6, and 10 μm were 6.75, 9.0, and 9.75 tube/μm^2, respectively. Also, SPICE calculation, or circuit simulation, was performed at each s-SWCNT network constituting an electrical path between source and drain electrodes of FET. In all channel lengths, On/Off ratio of s-SWCNT networks was enhanced with the increase of network density. Finally, we found a power law relationship between On/Off ratio of s-SWCNT networks and network density at percolation threshold.

Introduction

Carbon nanotube (CNT) has been paid much attention as an electronic material due to outstanding electrical properties since its discovery in 1991.[1,2] In general, it has been known that according to its chirality, electrical properties of CNT can be classified into two types: metallic and semiconducting ones.[3-7] Depending on applications, CNT is used in various fields such as organic light-emitting diode, transparent conductive film, and solar cell.[8-10] In this case, CNT networks are preferred to an individual CNT. This is because treating CNT as a structure of networks is convenient for further applications, compared with an individual CNT.

Actually, it is possible to use highly pure semiconducting or metallic CNT by virtue of a progressive advance in CNT separation techniques. Single-walled carbon nanotube (SWCNT) was sorted by diverse methods such as sequence-dependent DNA assembly, gel-based separation, density differentiation.[11-13] Also, direct synthesis for semiconducting SWCNT (s-SWCNT) has been reported.[14] These methods stimulated CNT electronics in basic and applied fields.

When CNT is utilized in electronics as the form of networks, an essential issue is the presence of an electrical path which is constituted by individual semiconducting or metallic CNT in the networks. Much effort has been made to study electrical percolation in CNT networks based on Monte Carlo method.[15-20] This approach can contribute to the improvement of finding an optimal condition in constituting CNT networks. Sangwan and co-workers optimized transistor performance of percolating CNT networks with help of Monte Carlo simulation.[18] Also, this approach can predict the effect of vacancy defects of CNT on electrical characteristics when the defective CNT constitutes networks. Berahman et al. calculated that CNT with double vacancy decreases electrical conductivity of percolated CNT network.[20] Furthermore, theoretical work can calculate electrical characteristics of CNT networks which have a different ratio of metallic and semiconducting CNT. It can give a guideline in designing experimental conditions to prepare

CNT networks. In spite of laborious efforts on CNT percolation, most of studies focused on multi-walled CNT or SWCNT networks where s-SWCNT exist with metallic SWCNT (m-SWCNT) at the same time. Percolation threshold of s-SWCNT networks has not been reported. In addition, most of previous works hardly studied electrical characteristics of percolated CNT networks. This motivated us to obtain percolation threshold of s-SWCNT and relate it to electrical characteristics.

In this study, we report on electrical percolation threshold of s-SWCNT networks formed in the channel of field-effect transistor (FET) and the electrical characteristics of percolated networks by using SPICE simulator. Actually, there are a number of experimental works where highly pure s-SWCNT networks were constituted between source and drain electrodes on FET for various purposes.[21-28] In the constitution of s-SWCNT networks with an impurity of m-SWCNT, we cannot expect semiconducting behaviour from dense s-SWCNT networks due to metallic path in the networks. To avoid this, the information on critical network density of s-SWNCT is required. However, to the best of our knowledge, the critical number of s-SWCNT has not been reported in constituting network at a given channel length, including electrical characteristics of the networks. Therefore, it is significant to theoretically calculate the critical number of s-SWCNT which is required to constitute networks at given channel length. For this reason, we calculated percolation threshold of s-SWCNT networks in the channel of FET and the electrical characteristics of the networks. Monte Carlo method was employed to generate random networks, and s-SWCNT networks were generated 100 times by varying network density at a given channel length to obtain percolation probability of s-SWCNT. Three channel lengths were used at a fixed channel width in calculations. Also, we did not restrict an angle of s-SWCNT with respect horizontal axis in random network generation. Relative neighbourhood graph (RNG) represents the morphology of percolated s-SWCNT networks quit well, so that we employed percolation threshold in RNG to gain electrical percolation threshold of s-SWCNT networks. Then, SPICE simulation was carried out to predict the electrical characteristics of the percolated s-SWCNT networks, and percolation threshold of s-SWCNT networks was related to electrical characteristics.

We think that our work can provide a theoretical guideline in constituting s-SWCNT networks at a given channel length of FET.

Computational procedure

To obtain the electrical percolation threshold of s-SWCNT networks, 2 dimensional (2D) networks of s-SWCNT were randomly distributed in the channel of FET. The networks were generated by MATLAB code based on Monte Carlo method. Fig. 1(a) shows a schematic illustration of a model system for 2D s-SWCNT networks on FET. The electrical percolation threshold was calculated at three different channel lengths of 2, 6, and 10 μm defined by source-drain electrodes. The channel

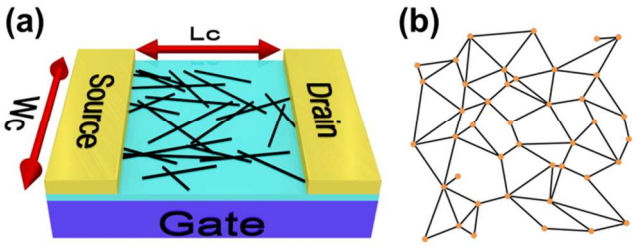

Fig. 1 (a) Schematic diagram of FET for percolation simulation of s-SWCNT networks. Sticks represent s-SWCNTs which constitute networks between source and drain electrodes on a dielectric layer of a substrate. Three different channel lengths (L_c, 2, 6, and 10 μm) were considered at a fixed channel width (W_c). (b) Illustration of RNG which represents percolated s-SWCNT networks quite well.

width was fixed to 2 μm in each calculation. Also, the length of s-SWCNT was 1 μm (standard deviation $\sigma = 0.1$) while the angle of s-SWCNT with respect to horizontal axis was randomly decided to be aligned to all direction during the generation of the networks. The length was determined by experimental results reporting that pure s-SWCNT has the centre at 1 μm in length distribution.[29,30] To analyze s-SWCNT networks with percolation theory, we employed bond percolation in RNG among diverse percolation models. It is because RNG seen in Fig. 2(b) is geometrically quite similar to 2D random networks of s-SWCNT. To acquire the percolation probability of s-SWCNT networks, network generation was conducted 100 times at different network density of channel length. In addition, the number of s-SWCNT for network density was carefully decided so that the probability is distributed from 0 to 1 at each channel length. We defined percolation threshold to be 0.77 because the bond percolation threshold of RNG has been reported to be 0.77.[32]

Then, NGSPICE calculation was carried out to relate percolation threshold of the networks to electrical characteristics of s-SWCNT networks. For this, the information on network percolation was converted to NGSPICE netlist file after finding connected electrical paths in the networks. In SPICE calculation, each s-SWCNT was modeled as simple p-type metal-oxide-semiconductor FET (MOSFET) since only s-SWCNT was considered in this study. The junction resistance between s-SWCNTs was carefully determined based on the experimental works on junction conductance between s-SWCNTs.[31] The study measured the junction conductance constituted by two individual s-SWCNTs to be $0.011e^2/h$ and $0.06e^2/h$ (where e is the electron charge and h is Planck's constant). From this, the junction resistances were calculated by inversing $0.011e^2/h$ and $0.06e^2/h$. As a result, the average of the calculated junction resistances was 1.4 MΩ, and this value was used in the SPICE simulation. Transfer characteristic curves of s-SWCNT networks were obtained by sweeping gate voltage from -3 to 3 V at fixed source-drain voltage of 1 V. On/Off ratio of the networks was calculated by the ratio of the maximum to minimum current in transfer characteristic curves when s-SWCNT constituted networks.

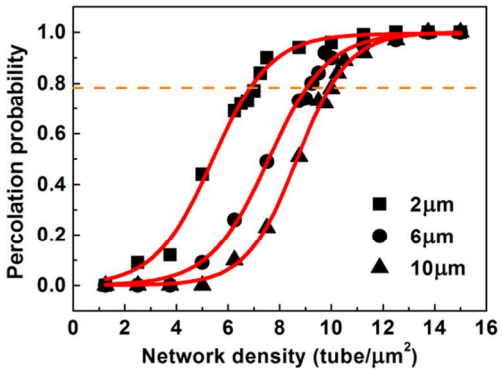

Fig. 2 Plot of percolation probability versus network density at channel length of 2, 6, and 10 μm. A dashed lined was put at percolation probability of 0.77 which corresponds to percolation threshold in RNG. The network density at percolation threshold increases with the increase of channel length.

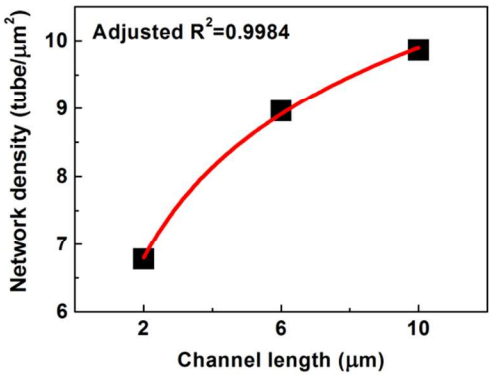

Fig. 3 Effect of network density at percolation threshold by channel length. The network density at percolation threshold increases with the increase of channel length.

Results and discussion

To obtain percolation probability at each channel length, we generated s-SWCNT networks 100 times by using Monte Carlo simulation at different network density of s-SWCNT. Fig. 2 shows the percolation probability of s-SWCNT networks with respect to network density at channel length defined by source-drain electrodes. Regardless of channel length, we can see a trend that percolation probability becomes low at sparse network density while it grows at high network density. However, the distribution of percolation probability has a different symmetry with respect to network density, depending on channel length. Hence, we fitted the obtained data to sigmoidal Boltzmann equation which has the following form:

$$y = \frac{(A_1 - A_2)}{[1+\exp(x - x_0)/\Delta x]} + A_2$$

where, y is percolation probability of s-SWCNT networks, x is the network density, A_1 is the initial value of y, A_2 is the final value of y and x_0 and $\triangle x$ are the centre and the width of the function, respectively. The fitting parameters are summarized in Table 1 with adjusted R^2 values. As seen in the table, all adjusted R^2 values are close to 1, meaning that the fitting to sigmoidal Boltzmann equation is quite appropriate. We can see in Fig. 2 that x_0 shifts to a region of high network density as the channel length increases. Especially, the table shows that an abrupt increase in x_0 occurs when channel length changes from 2 to 6 μm. Despite we considered the same interval for channel length, this value is greater than the difference between 6 and 10 μm. It can be attributed to the length of s-SWCNT (1 μm) considered in this work. Since the length of individual s-SWCNT is the half of the channel length in the case of 2 μm, the percolation probability of s-SWCNT networks increases even at a small number of s-SWCNT, leading to sparse network density. On the other hand, the channel lengths of 6 and 10 μm are 6 and 10 times longer than the length of s-SWCNT, respectively. In both cases, a large number of s-SWCNT is stochastically required to constitute s-SWCNT networks, compared with 2 μm. This is the reason why x_0 shifts to the right in the axis of network density as the channel length increases.

Table 1 Fitting parameters for sigmoidal Boltzmann analysis at each channel length.

	2 μm	6 μm	10 μm
A_1	0	0	0
A_2	0.9945	0.9982	1.0
X_0	5.3964	7.5657	8.6672
$\triangle x$	1.1157	1.1461	0.9876
Adjusted-R^2	0.9927	0.9967	0.9980

To gain percolation threshold at each channel length, we employed bond percolation in RNG which represents the morphology of s-SWCNT percolation well. Percolation threshold in RNG has been reported to be 0.77.[32] Hence, as shown in Fig. 2, we plotted a dashed line at a value of 0.77 in the axis of percolation probability. The network densities at percolation threshold, calculated from sigmoidal Boltzmann equation in the channel of 2, 6, and 10 μm, were 6.75, 9.0, and 9.75 tube/μm^2, respectively. To know the relationship between network density and channel length, we plotted network density at percolation threshold against channel length in Fig. 3. The figure shows that as channel length increases, network density corresponding to percolation threshold of s-SWCNT networks increases logarithmically. As explained before, network density of s-SWCNT abruptly increases when channel length increases from 2 to 6 μm. This can be explained as following: junctions

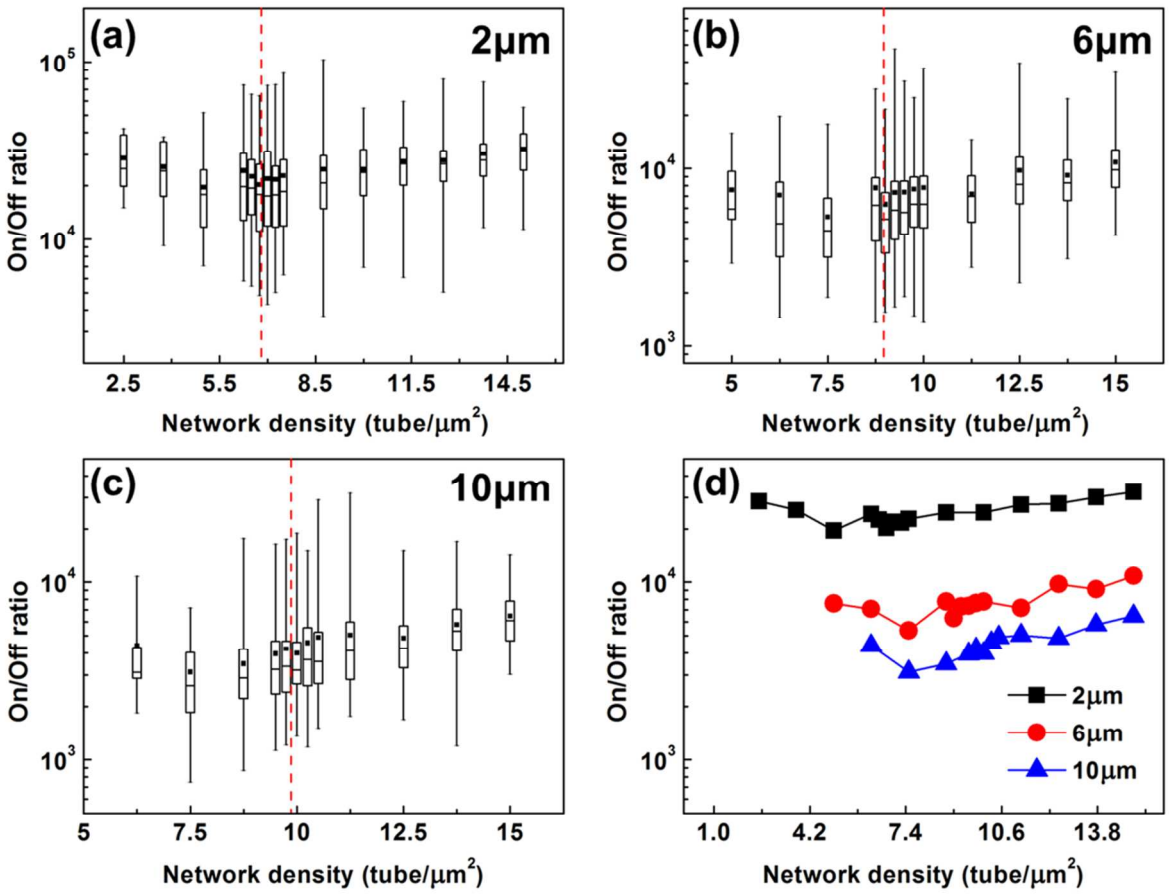

Fig. 4 Box plot of On/Off ratio of percolated s-SWCNT networks versus network density at channel length of (a) 2, (b) 6, and (c) 10 μm. On/Off ratio is enhanced in all cases as network density increases. Average On/Off ratio of percolated s-SWCNT is summarized with respect to network density as shown in (d). Square, circle, and triangle represent the change of average On/Off ratio with respect to network density at channel length of 2, 6, and 10 μm, respectively.

in the channel of FET can be classified into s-SWCNT to electrode and s-SWCNT to s-SWCNT contacts. When s-SWC NT contacts with electrode in FET, it is a junction between one- and two-dimensional structures. Meanwhile, the contact between s-SWCNT to s-SWCNT is a junction constituted by one-dimensional structures. In general, we can predict a higher probability in the contact between one- and two-dimensional structures than the contact between one-dimensional ones. Therefore, the percolation probability of forming networks becomes low as channel length increases. In other words, more s-SWCNTs are required to compensate the low contact probability between s-SWCNTs, covering the increased area by the extension of channel length.

After generating s-SWCNT networks at each channel length, transfer characteristics were obtained from percolated s-SWCNT networks by SPICE simulator. At each channel, On/Off ratio of FET was calculated from all percolated networks and the results were displayed in Fig. 4 (a), (b), and (c) as box plot form against network density. A dotted line was put at the network density corresponding to percolation threshold of s-SWCNT networks, and average On/Off ratio was marked with closed square in all cases. At any case, we can see that On/Off ratio is enhanced as network density increases. This result is different from the previous results, where m-SWNCT and s-SWCNT co-exist in percolated networks.[33] In the co-existence of s-SWCNT and m-SWCNT, On/Off ratio rapidly decreases at dense SWCNT networks due to metallic path by m-SWCNT. The m-SWCNT path becomes electrically dominant one in SWCNT networks when voltage is applied. Therefore, we cannot expect a semiconducting behavior originated from percolated s-SWCNT networks.

In the case of 2 μm (Fig. 4(a)), we can notice that the difference between the maximum and the minimum of On/Off ratio gradually decreases above percolation threshold. This is because percolation probability approaches to 1 by the increase in the number of s-SWCNT, leading to narrow distribution of On/Off ratio. Fig. 4(b) exhibits the box plot corresponding to the channel length of 6 μm. It seems that the difference between the maximum and the minimum is not too large, compared with that shown in Fig. 4(a). Also, we can see that On/Off ratio is slightly enhanced with the increase of network density. However, the box plot of 10 μm shows a different trend that the difference between the maximum and the minimum of On/Off ratio varies unevenly with the increase of network density. It is

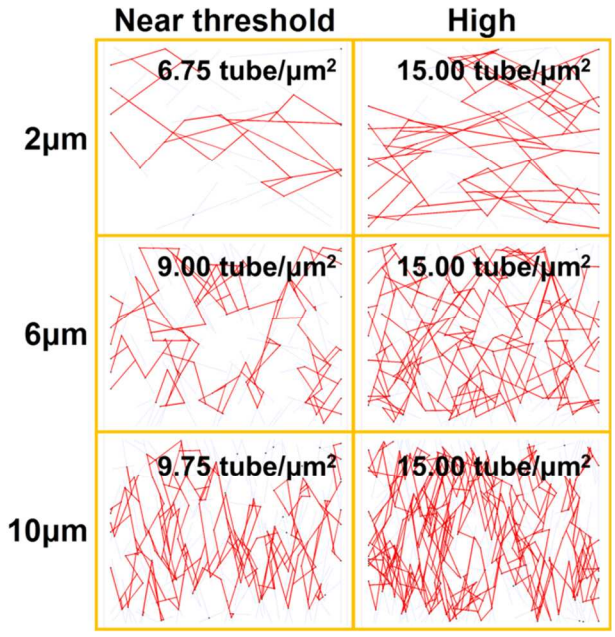

Fig. 5 Representative percolation morphologies of s-SWCNT networks at different channel length and network density. The increase in network density as well as channel length leads to the increased number of an electrical path and contact junction.

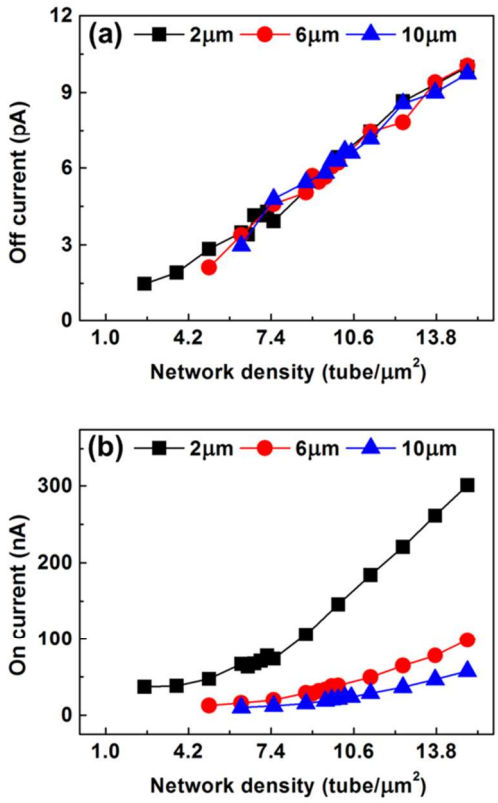

Fig. 6 Plot of average (a) Off-state and (b) On-state current versus network density at channel length of 2 (square), 6 (circle), and 10 μm (triangle).

because the extended channel length gives high probability that percolated networks have a different number of junctions and paths in spite of high network density. To investigate the effect of network density on On/Off ratio, we plotted average On/Off ratio of all channels in the same figure as exhibited in Fig. 4(d). As shown in the figure, On/Off ratio slightly increases above percolation threshold in all cases with the increase of network density. Therefore, we can conclude that On/Off ratio has a proportional relationship to network density of s-SWCNT. Meanwhile, In Fig. 4(d), we can notice that On/Off ratio is decreased as channel length increases. The figure indicates that when channel length is 2 μm, we can expect On/Off ratio of more than 10^4 regardless of network density. On the other hand, On/Off ratio has the value between 10^3 and 10^4 when the channel length is greater than 2 μm. Based on this result, it can be deduced that On/Off ratio of s-SWCNT is dependent on the channel length of FET.

In general, the value of On/Off ratio can be determined by dividing the maximum of On-state current by the minimum of Off-state one. And, the current from s-SWCNT networks is influenced by the number of junction and an electrical path in the networks. Therefore, the investigation of percolation morphology of s-SWCNT is significant to compare the difference in the number of junction at different channel lengths and network densities. In Fig. 5, we illustrated representative percolation morphologies selected near threshold network density and from the region of high network density. The number of an electrical path in the percolated networks commonly increases in all channel lengths as the networks become dense. At the fixed network density, the number of junction increases in proportion to channel length as shown in Fig. 5. This increase leads to the enhancement of junction resistance in the s-SWCNT networks and influences On- and Off-state current of FET.

Hence, we analyzed average On-state current and Off-state current in all cases to clarify the dependency of On/Off ratio on channel length. Fig. 6 (a) and (b) exhibit a plot of average Off-state and On-state current with respect to network density of s-SWCNT, respectively. Interestingly, it seems that Off-state current is not affected by channel length and holds a similar value regardless of channel length as seen in Fig. 6(a). In all channel lengths, Off-state current linearly increases in proportion to network density. It can be interpreted that the resistance of an individual s-SWCNT is much higher than junction resistance and that the effect of junction resistance is insignificant. On the other hands, Fig. 6(b) evidently shows that On-state current decreases as the channel length increases. It can be attributed to the junction resistance of s-SWCNT networks. As channel length increases, the number of s-SWCNT also increases to constitute an electrical path between the source-drain electrodes of FET. This means that the number of junction in the networks also increases by extending channel length. Therefore, a longer channel contributes to the enhancement of junction resistance and this makes the On-state

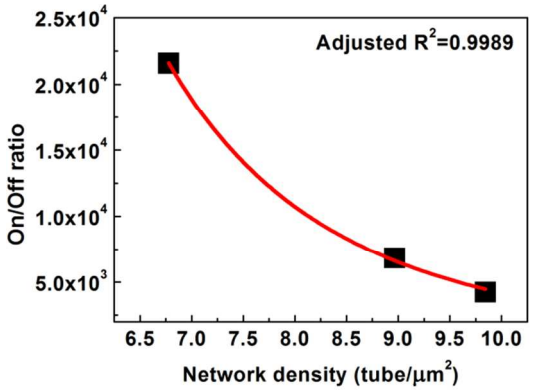

Fig. 7 Relationship between average On/Off ratio and network density corresponding to percolation threshold of s-SWCNT at each channel. At percolation threshold, On/Off ratio of s-SWCNT networks drastically decreases with respect to network density.

current decrease. As a result, On/Off ratio is decreased with the increase of channel length.

Next, we investigated a relationship between percolation threshold and electrical characteristics at each channel length. As an analytic variable, we selected network density at percolation threshold of 0.77 in all channel lengths. Also, average On/Off ratio was selected as a variable for electrical characteristics of s-SWCNT networks. Fig. 7 exhibits a change of average On/Off ratio with respect to network density at percolation threshold. The following formula was employed for the relationship between average On/Off ratio and the network density:

$$(\mathrm{On/Off})_{\mathrm{avg}} = \mathrm{b} \times (\mathrm{Network\ density})^{\mathrm{a}}$$

A power law model was used to fit the data and the fitting parameters of a and b were -4.22 and 7.0×10^7, respectively. The value of adjusted R^2 was 0.9989 which is close to 1. It indicates that On/Off ratio is strongly influenced by the network density at percolation threshold. On/Off ratio drastically decreases as the network density at percolation threshold in each channel length increases. Especially, in spite of the same interval of channel length, a sudden decrease in On/Off ratio occurs between the network densities corresponding to percolation threshold of 2 and 6 μm. It can be demonstrated that at percolation threshold of each channel, more s-SWCNTs are necessary to constitute networks between electrodes with the increase of channel length. Simultaneously, the number of junction between s-SWCNTs grows in s-SWCNT networks, leading to the enhancement of junction resistance. Finally, low On/Off ratio is obtained from s-SWCNT networks formed in extended channel length. To analyze our result, the theory of MOSFET model was employed. When MOSFET is switched on, drain current (I_D) generally depends on the channel dimension of channel length and channel width. In this study, channel width is fixed to 2 μm in all cases.

$$I_D \propto \frac{\text{Channel width}}{\text{Channel length}}$$

Therefore, we can see that I_D has an inversely proportional relationship to channel length. On the other hand, I_D is not influenced by channel dimension when MOSFET is switched off. From the relationship, we can expect that On/Off ratio decreases inversely proportional to channel length. As shown in Fig. 7, our result is consistent with MOSFET model.

Conclusions

In this work, we theoretically obtained percolation threshold of s-SWCNT networks at different channel length on the basis of Monte Carlo method. As a result, percolation thresholds of s-SWCNT were calculated to be 6.75, 9.0, and 9.75 tube/μm^2 when channel lengths are 2, 6, and 10 μm. Network density which was gained at percolation threshold of s-SWCNT increased with respect to channel length. In addition, we predicted the electrical characteristics of percolated s-SWCNT networks at each channel length by using SPICE simulator. It was revealed that On/Off ratio was slightly enhanced with the increase of network density in all channel lengths. Finally, we found a power law relationship between On/Off ratio and network density at percolation threshold of s-SWCNT. It was originated from the reduction of On-state current due to the enhanced junction resistance by extending channel length of FET.

This study can provide a theoretical guideline in constituting CNT networks as well as s-SWCNT networks at a given channel length of FET.

Acknowledgements

This work was supported by BK21 Humanware Information Technology and the Center for Advanced soft Electronics under the Global Frontier Research Program of the Ministry of Education (No. 2011-0031638).

Notes and references

School of Electrical Engineering, Korea University, Anam-dong, Seongbuk-gu, 136-713 Seoul, Korea. E-mail: nanotube@korea.ac.kr; Tel: +82-2-3290-3801

1 S. Iijima, *Nature*, 1991, **354**, 56-58.
2 X. Zhou, J.-Y. Park, S. Huang, J. Liu and P. L. McEuen, *Phys. Rev. Lett.*, 2005, **95**, 146805.
3 J. W. Mintmire, B. I. Dunlap and C. T. White, *Phys. Rev. Lett.*, 1992, **68**, 631-634.
4 R. Saito, M. Fujita, G. Dresselhaus and M. S. Dresselhaus, *Phys. Rev. B*, 1992, **46**, 1804-1811.

5 N. Hamada, S.-I. Sawada and A. Oshiyama, *Phys. Rev. Lett.*, 1992, **68**, 1579-1581.
6 B. I. Dunlap, *Phys. Rev. B*, 1994, **49**, 5643-5650.
7 M. Menon, E. Richter and K. R. Subbaswamy, *J. Chem. Phys.*, 1996, **104**, 5875-5882.
8 D. Zhang, K. Ryu, X. Liu, E. Polikarpov, J. Ly, M. E. Tompson and C. Zhou, *Nano Lett.*, 2006, **6**, 1880-1886.
9 B. Dan, G. C. Irvin and M. Pasquali, *ACS Nano*, 2009, **3**, 835-843.
10 R. Ulbricht, S. B. Lee, X. Jiang, K. Inoue, M. Zhang, S. Fang, R. H. Baughman and A. A. Zakhidov, *Sol. Energy Mater. Sol. Cells*, 2007, **91**, 416-419.
11 M. Zheng, A. Jagota, M. S. Strano, A. P. Santos, P. Barone, S. G. Chou, B. A. Diner, M. S. Dresselhaus, R. S. McLean, G. B. Onoa, G. G. Samsonidze, E. D. Semke, M. Usrey and D. J. Walls, *Science*, 2003, **302**, 1545-1548.
12 T. Tanaka, H. Jin, Y. Miyata, S. Fujii, H. Suga, Y. Naitoh, T. Minari, T. Miyadera, K. Tsukagoshi and H. Kataura, *Nano Lett.*, 2009, **9**, 1497-1500.
13 M. S. Arnold, A. A. Green, J. F. Hulvat, S. I. Stupp and M. C. Hersam, *Nature Nanotech*., 2006, **1**, 60-65.
14 L. Qu, F. Du and L. Dai, *Nano Lett*., 2008, **8**, 2682-2687.
15 J. Li, Z.-B. Zhang and S.-L. Zhang, *Appl. Phys. Lett.*, 2007, **91**, 253127.
16 F. Du, J. E. Fischer and K. I. Winey, *Phys. Rev. B*, 2005, **72**, 121404.
17 S. Pfeifer, S.-H. Park and P. R. Bandaru, *J. Appl. Phys.*, 2010, **108**, 024305.
18 V. K. Sangwan, A. Behnam, V. W. Ballarotto, M. S. Fuhrer, A. Ural and E. D. Williams, *Appl. Phys. Lett.*, 2010, **97**, 043111.
19 B. Chandra, H. Park, A. Maarouf, G. J. Martyna and G. S. Tulevski, *Appl. Phys. Lett.*, 2011, **99**, 072110.
20 M. Berahman, M. Taheri, M. H. Sheikhi and A. Zarifkar, Electrical Engineering (ICEE), 21st Iranian Conference on, Mashhad, 14–16 May, 2013, DOI: 10.1109/IranianCEE.2013.6599543.
21 N. Izard, S. Kazaoui, K. Hata, T. Okazaki, T. Saito, S. Iijima and N. Minami, *Appl. Phys. Lett.*, 2008, **92**, 243112.
22 D.-H. Kim, J. K. Lee, J. H. Huh, Y. H. Kim, G. T. Kim, S. Roth and U. Dettlaff-Weglikowska, *Phys. Status Solidi B*, 2011, **248**, 2668-2671.
23 D.-H. Kim, S. Y. Lee, J. E. Jin, G. T. Kim and D.-J. Lee, *Phys. Chem. Chem. Phys.*, 2014, **16**, 6980-6985.
24 D.-H. Kim, J. E. Jin, M. Piao, J. H. Choi and G. T. Kim, *Phys. Chem. Chem. Phys.*, 2014, **16**, 18370-18374.
25 S. Fujii, T. Tanaka, Y. Miyata, H. Suga, Y. Naitoh, T. Minari, T. Miyadera, K. Tsukagoshi and H. Kataura, *Appl. Phys. Express*, 2009, **2**, 071601.
26 S. K. Raman Pillai and M. B. Chan-Park, *ACS Appl. Mater. Interfaces*, 2012, **4**, 7047-7054.
27 K. C. Narasimhamurthy and P. Roy, *Semicond. Sci. Technol.*, 2011, **26**, 075002.
28 K. C. Narasimhamurthy and R. Paily, *Solid State Electron.*, 2013, **79**, 37-44.
29 B. K. Sarker, S. Shekhar and S. I. Khondaker, *ACS Nano*, 2011, ***5***, 6297–6305.
30 C. Wang, J. Zhang and C. Zhou, *ACS Nano*, 2010, **4**, 7123–7132.
31 M. S. Fuhrer, J. Nygård, L. Shih, M. Forero, Y.-G. Yoon, M. S. C. Mazzoni, H. J. Choi, J. Ihm, S. G. Louie, A. Zettl and P. L. McEuen, *Science*, 2000, **288**, 494-497.
32 O. Melchert, *Phys. Rev. E*, 2013, **87**, 042106.
33 J. Li, Z.-B. Zhang and S.-L. Zhang, *Appl. Phys. Lett.*, 2007, **91**, 253127.